

DAMAGING OF PURE TUNGSTEN WITH DIFFERENT MICROSTRUCTURE UNDER SEQUENTIAL QSPA AND LHD PLASMA LOADS

S.S. Herashchenko^{1,2}, O.V. Byrka¹, V.A. Makhraj^{1,2}, M. Wirtz³, N.N. Aksenov¹, I.E. Garkusha^{1,2}, Yu.V. Petrov¹, S.V. Malykhin⁴, S.V. Surovitskiy⁴, S. Masuzaki⁵, M. Tokitani⁵, S.I. Lebedev¹, P.B. Shevchuk¹

¹ *Institute of Plasma Physics NSC “Kharkov Institute of Physics and Technology”, Kharkiv, Ukraine;*

² *V.N. Karazin Kharkiv National University, Kharkiv, Ukraine;*

³ *Forschungszentrum Julich, EURATOM Association, Julich, Germany;*

⁴ *National Technical University “Kharkiv Polytechnic Institute”, Kharkiv, Ukraine;*

⁵ *National Institute for Fusion Science, Oroshi 322-6, Toki 509-5292 JAPAN*

E-mail: gerashchenko@kipt.kharkov.ua

The cracking thresholds were evaluated for tungsten samples with different microstructure in the course of QSPA Kh-50 repetitive plasma loads. No damage has been observed on the exposed surfaces under 0.1 MJ/m². Nevertheless, cracks were detected in the bulk of irradiated tungsten (with longitudinal grain orientation). Increasing heat load up to 0.2 MJ/m² caused the damaging of all types of tungsten targets. The observed cracks propagate to the bulk mainly transversely and parallel to the irradiated surface. The effect of the subsequent exposure with LHD divertor plasma on the tungsten samples was analyzed. The obtained results are discussed.

PACS: 52.40.Hf

INTRODUCTION

Tungsten is now considered as a primary material for the armor of plasma facing components in the divertor region of fusion devices like ITER and DEMO. The development of advanced tungsten grades requires thorough testing and qualification of material in extreme fusion relevant conditions, including both high heat and particle fluxes (H isotopes, He and neutron) [1, 2].

Experimental simulations of high-energy fluxes expected in fusion reactors are carried out in presently available fusion devices such as ASDEX Upgrade, JET or Large Helical Device (LHD) [1, 3]. Furthermore, simulation experiments are also performed using linear and e-beam facilities, pulsed plasma guns, powerful quasi-stationary plasma accelerators (QSPA) as test-bed facilities [4-13].

For pure tungsten as well as for tungsten-based composites the surface cracking has been extensively studied within the linear plasma devices and e-beam facilities [11-13]. The obtained results showed different kinds of damage appeared depending on the loading sequence, power density, microstructure of the samples, and their base temperature. W samples with transversal grain orientation exhibited the weakest damage resistance and the increase of their base temperature could not compensate for the detrimental impact of deuterium. It is shown that transient heat load led to the appearance of surface crack meshes, while consecutive steady-state load induced tensile stresses and opened existing surface cracks [13].

Incident helium ions might also have a strong impact on the surface evolution, with the formation of dislocation loops and bubbles [1, 12]. These changes at the material surface might promote the hydrogen

retention in the structure, which is one of the major concerns for next generation devices. Therefore, understanding of the microstructure changes and its consequences are of primary importance. Microscopic damage and helium depth profiles in metals bombarded by helium atoms have been studied during LHD helium discharges. From TEM observations, a considerable amount of dislocation loops and helium bubbles of about 1...2 nm size are identified [3, 14].

The observation of micro-crack networks in experiments involving QSPA Kh-50 was attributed to the surface melting and subsequent re-solidification [5, 15]. It was found that due to the material degradation, the increasing number of repetitive exposures shifts down the energy threshold for the crack onset up to 50 percent [15-17]. Even the loads, which are twice less than the melting energy threshold led to the appearance of fatigue cracks already after 100 plasma pulses. In this case, the cracks initiation could be caused by an accumulation of the stress-induced lattice defects which harden the material in plasma-affected thin sub-surface layer [7-9]. Analysis of experimental data confirms that the origin of crack formation could be attributed to the plastic deformation of surface layers by the twinning mechanism. The twinning mechanism is reinforced by the interaction of twins with hydrogen-filled micro-pores [8, 9].

Thus, experiments with sequential transient and stationary heat loads have shown quite a strong influence of combined impact on plasma facing materials. Therefore, further evaluation of damaging thresholds for tungsten in conditions of combined heat loads relevant to fusion reactor is necessary. This paper presents the first results on sequential moderate pulsed plasma loads from the QSPA Kh-50 plasma accelerator

and following exposures of as-received and pretreated samples by ions and charge-exchange particles within the divertor fluxes in the Large Helical Device.

1. EXPERIMENTAL SETUP AND DIAGNOSTICS

Plasma-heat load tests of tungsten with energy density, pulse duration and particle loads relevant to ITER transient events have been carried out in a QSPA Kh-50 quasi-stationary plasma accelerator [5, 6]. Samples of pure tungsten with the longitudinal (L) and transversal (T) grain orientation and in the recrystallized (R) state were used for the experiments [13]. Samples have sizes of $(12 \times 12 \times 5) \text{ mm}^3$. All specimens were polished to achieve a mirror-like surface. The samples were supplied by Plansee AG, prepared and delivered from Forschungszentrum Julich.

The main parameters of the QSPA Kh-50 plasma streams were as follows: ion impact energy $\sim 0.4 \text{ keV}$; maximum plasma pressure up to 0.32 MPa ; the plasma stream diameter 18 cm . The plasma pulse shape is triangular with pulse duration of 0.25 ms [15]. The heat loads onto the exposed surfaces were selected to be rather moderate: $0.1 \text{ MJ} \cdot \text{m}^{-2}$ (heat flux factor $F_{\text{HF}} \approx 6.3 \text{ MW} \cdot \text{s}^{0.5} \cdot \text{m}^{-2}$) and $0.2 \text{ MJ} \cdot \text{m}^{-2}$ ($F_{\text{HF}} \approx 12.7 \text{ MW} \cdot \text{s}^{0.5} \cdot \text{m}^{-2}$) to operate below the tungsten cracking threshold for a small number of plasma pulses [15]. Before each plasma pulse, the surface temperature (T_{base}) of one series of tungsten targets was kept near room temperature (RT). The second series of the samples was preheated before the exposures to $T_{\text{base}} = 400^\circ\text{C}$ with a special heater [5, 16]. The maximum number of irradiation plasma pulses was 200.

The induced damages have been analyzed by SEM and laser profilometry after 100 and 200 the QSPA pulses. Subsequently, the cross sections of the samples have been investigated by metallographic means to analyze the crack propagation into the bulk material.

As the second step, an irradiation of both pre-loaded and original W targets was performed by deuterium plasma fluxes (average ion flux of $3.7 \cdot 10^{23} \text{ m}^{-2} \cdot \text{s}^{-1}$, heat flux of $\leq 10 \text{ MW/m}^2$) at the divertor region within Large Helical Device (LHD) at the National Institute of Fusion Science [3, 14]. The samples were exposed to the divertor plasma fluxes for 2 s . Subsequently the irradiated samples were analyzed using SEM+EDS, and TEM (transmission electron microscopy).

2. EXPERIMENTAL RESULTS

2.1. TUNGSTEN SAMPLES EXPOSED WITH HEAT LOAD TO 0.1 MJ/m^2

Samples of pure tungsten (longitudinal (L) and transversal (T) grain orientation and in the recrystallized state (R)) were exposed to 100 and 200 QSPA plasma pulses with heat load $0.1 \text{ MJ} \cdot \text{m}^{-2}$ (heat flux factor $F_{\text{HF}} \approx 6.3 \text{ MW} \cdot \text{s}^{0.5} \cdot \text{m}^{-2}$).

Plasma irradiation after 100 QSPA pulses with a surface heat load of 0.1 MJ/m^2 does not cause damages on the exposed surfaces of all tungsten samples

independently on their microstructure (Fig. 1). Only slightly increasing surface roughness is observed ($R_a \leq 1.2 \mu\text{m}$). The metallographic analysis shows the cracks penetration to the bulk of exposed tungsten sample with longitudinal orientation (Fig. 2). The cracks propagate to the material in parallel to the sample surface. The maximum crack depth is about $200 \mu\text{m}$.

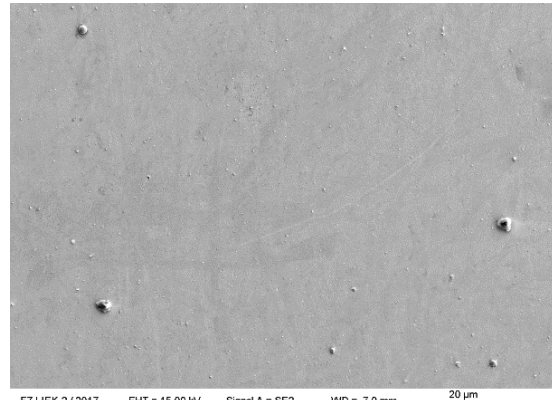


Fig. 1. SEM image of L sample surface exposed with the QSPA plasma load of 0.1 MJ/m^2 at $T_{\text{base}} = 400^\circ\text{C}$



Fig. 2. Optical microscope image of the crack penetration in the metallographic cross section of L sample exposed with the plasma load of 0.1 MJ/m^2 at $T_{\text{base}} = 400^\circ\text{C}$

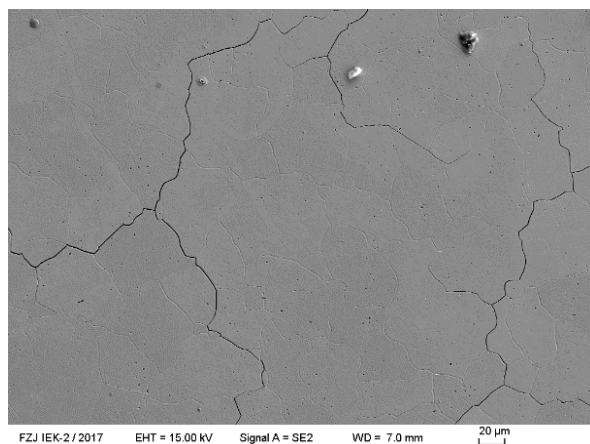


Fig. 3. SEM image of R sample surface after the QSPA exposure with heat load of 0.2 MJ/m^2 at $T_{\text{base}} = \text{RT}$

An increasing number of QSPA plasma exposures up to 200 pulses does not significantly affect the

samples' surface morphology. The metallographic analysis results are completely identical in both cases.

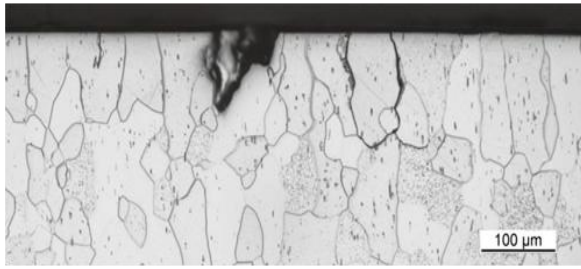


Fig. 4. Light microscope image of the metallographic cross section of R sample irradiated by the QSPA plasma load of 0.2 MJ/m^2 at $T_{base} = RT$

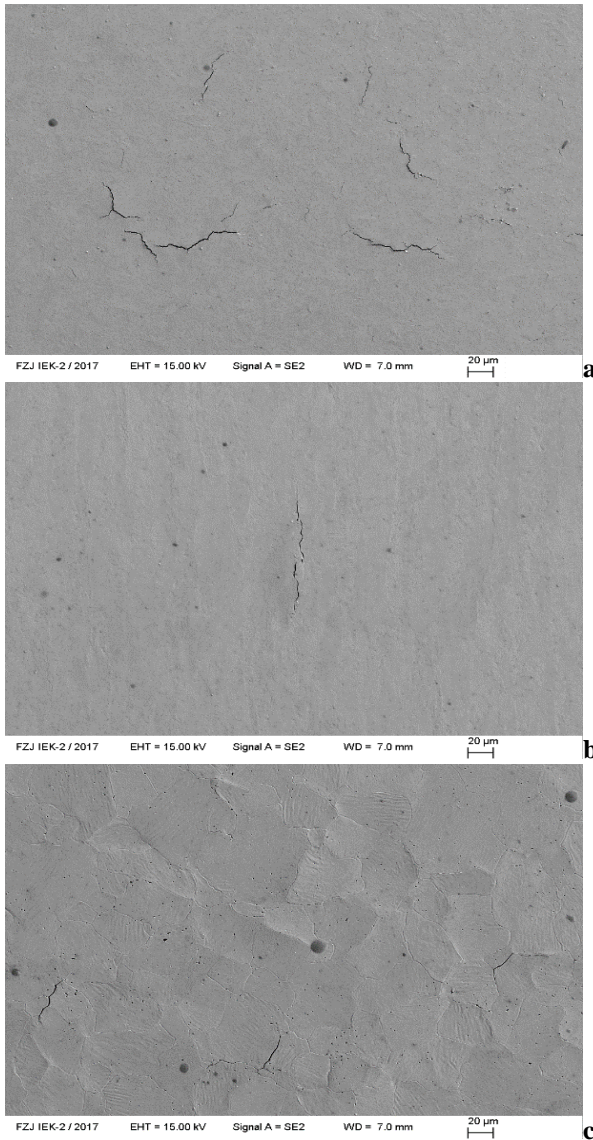


Fig. 5. SEM image of surface of T (a), L (b) and R (c) sample after the QSPA exposure with heat load of 0.2 MJ/m^2 at $T_{base} = 400^\circ\text{C}$

2.2. TUNGSTEN SAMPLES EXPOSED TO 0.2 MJ/m^2

Increasing heat load up to 0.2 MJ/m^2 causes surface damage appearance for all types of tungsten targets. A large number of repetitive plasma loads

($F_{HF} \approx 12.7 \text{ MW} \times \text{s}^{0.5} \times \text{m}^{-2}$) leads to surface modification and cracks appearing on affected surfaces.

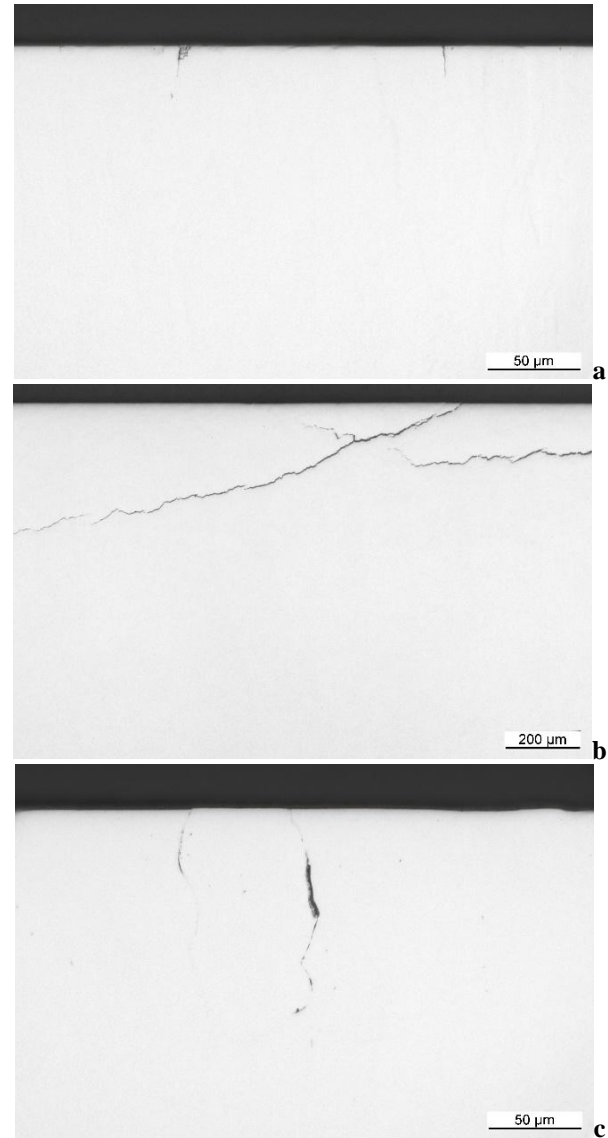


Fig. 6. Light microscope image of the metallographic cross section of T (a), L (b) and R (c) sample after the QSPA exposure with heat load of 0.2 MJ/m^2 at $T_{base} = 400^\circ\text{C}$

A rather significant difference has been observed in the morphology of tungsten samples that exposed at room temperature. Metallographic analysis for the recrystallized tungsten sample showed the formation of a network of cracks on the surface (Fig. 3). Crack propagation to the bulk along the grains boundaries is also observed at depths up to $150 \mu\text{m}$ (Fig. 4). For W samples with the longitudinal and transversal grain orientation, there were still no damages detected.

Small cracks were appeared on the surfaces of exposed tungsten samples pre-heated to 400°C (Fig. 5). The length of the cracks is varied from 30 to $80 \mu\text{m}$. Increasing surface roughness is observed for all samples too.

For tungsten samples with transversal grain orientation, single cracks propagate normally to the

surface. They are observed in the near-surface layer at depth of up to 50 μm (Fig. 6,a).

Features of the pre-heated L tungsten samples need to be discussed in more detail. As it is seen from the metallographic cross section (Figs. 2, 6,b), QSPA exposures with heat load of 0.1 MJ/m^2 and 0.2 MJ/m^2 lead to crack propagation in the near-surface layer parallel to the surface. Deep cracks are longer ($> 1\text{mm}$) in both cases. The maximum depth of cracks was almost 200 μm for the heat load of 0.1 and 600 μm for 0.2 MJ/m^2 . All cracks originate in the near-surface layer and further grow far into depth. Cracks change their orientation during propagation deviating from their initial path.

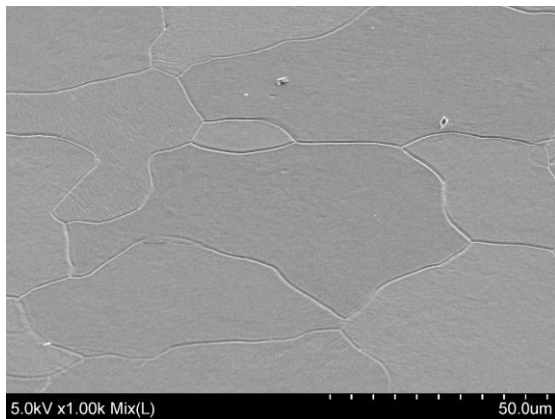


Fig. 7. SEM image of surface of R sample after the QSPA exposure and plasma fluxes in divertor region of LHD

2.3. TUNGSTEN SAMPLES EXPOSED TO THE LHD DIVERTOR PLASMA

Three types of tungsten samples (T, L, R) were further exposed to plasma fluxes in the divertor region of LHD both in as-received state and after the pulsed QSPA plasma loads (200 pulses of 0.1 MJ/m^2) aiming at analysis of possible effects from combined exposures.

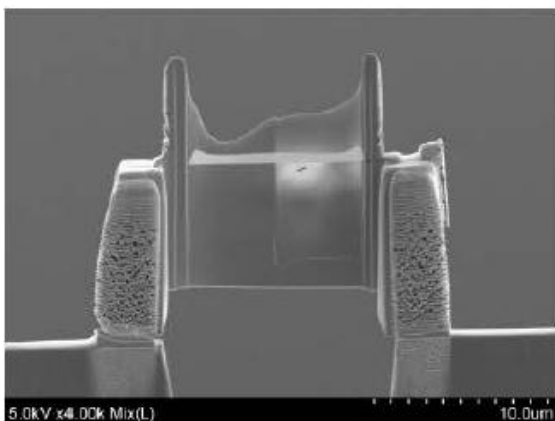


Fig. 8. TEM probe of R sample surface exposed to both QSPA plasma and divertor fluxes in LHD

The LHD divertor plasma exposures do not revealed any synergistic effects on the surfaces of the samples. Generally, no differences are observed on the surfaces between initial samples and ones irradiated by the QSPA Kh-50.

Analysis of the surface morphology of the tungsten samples indicates the absence of any extra damages. The grains' boundaries are clearly visible (Fig. 7).

After plasma exposures, microstructures of samples were observed by means of TEM. Fig. 8 presents the TEM probe from the R sample after the consecutive combination of the QSPA exposure and plasma fluxes in the LHD divertor.

It should be noted that LHD divertor fluxes resulted in surface modification and formation of a sub-surface layer of approximately 10 nm thickness for all exposed samples. In this layer, so-called bubbles are routinely observed (Fig. 9). Taking into account the sizes of bubbles, these bubbles look to be attributed to deuterium and helium bombardment effects within LHD.

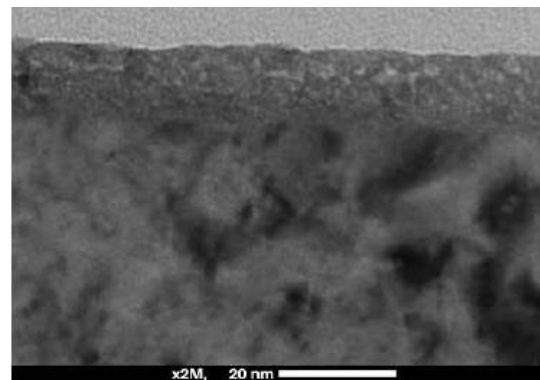


Fig. 9. TEM image of the cross section of R tungsten sample after the QSPA exposure and divertor plasma fluxes in LHD

CONCLUSIONS

Experimental studies of the damage features for pure tungsten with different microstructure under the moderate plasma loads have been performed with a quasi-stationary plasma accelerator QSPA Kh-50. The heat loads on the surface were below the cracking threshold (for virgin material). The number of plasma pulses was 100 and 200.

The repetitive plasma loads lead to surface modification and cracks appearing on affected surfaces. The influence of initial microstructure on tungsten damaging is clearly demonstrated.

No remarkable damage was observed on the exposed surfaces under 0.1 MJ/m^2 loads. Nevertheless, the cracks are found to be propagating in the bulk of exposed tungsten with longitudinal grain orientation.

Increasing heat load up to 0.2 MJ/m^2 causes the damaging of all types of tungsten targets. Depending on W material grade, the observed isolated cracks propagate to the bulk transversely and parallel to the exposed surface.

Except for some isolated cracks, no crack networks are observed on the exposed surfaces under the abovementioned plasma heat loads.

An effect of the LHD divertor plasma exposure on the surfaces of the tungsten samples was analyzed. LHD divertor fluxes are contributed to surface modification and formation of the sub-surface layer of approximately

10 nm in thickness for all exposed samples. In this layer, bubbles are found to be formed. Analysis of the sizes of bubbles suggests that these bubbles might be attributed to deuterium and helium effects in the LHD exposures.

For the case of moderate transient loads applied, the LHD divertor plasma exposures do not reveal any synergistic effects on the surfaces of the samples, which pre-damaged by the QSPA Kh-50. Influences of stronger cracking damage and also melting and resolidification effects from QSPA pulses on material performance in the divertor region are planned to be analyzed in our next step experiments.

ACKNOWLEDGEMENTS

This work has been carried out within the framework of the EUROfusion Consortium and has received funding from the Euratom research and training programme 2014-2018 and 2019-2020 under grant agreement № 633053. The views and opinions expressed herein do not necessarily reflect those of the European Commission.

This work has also been supported by National Academy Science of Ukraine projects X-2-11-10/2020 and П-2/24-2020.

REFERENCES

1. S. Brezinsek et al. // *Nuclear Fusion*. 2017, v. 57, p. 116041.
2. T. Hirai et al. // *Nuclear Materials and Energy*. 2016, v. 9, p. 616-622.
3. Q. Zhou et al. // *Fusion Engineering and Design*. 2020, v. 159, p. 111879.
4. S. Pestchanyi et al. // *Fusion Eng. Design* 2011, v. 86, 9-11, p. 1681-1684.
5. I.E. Garkusha et al. // *Fusion Science and Technology*. 2014, v. 65(2), p. 186-193.
6. V.A. Makhlay et al. // *Physica Scripta*. 2020, v. T171, p. 014047.
7. A. Bakaeva et al. // *Journal of Nuclear Materials*. 2019, v. 520, p. 185-192.
8. S.V. Malykhin et al // *Nuclear Inst. and Methods in Physics Research B*. 2020, v. 481, p. 6-11
9. S.S. Herashchenko et al. // *Nuclear Inst. and Methods in Physics Research B*. 2019, v. 440, p. 82-87.
10. A.A. Shoshin et al. // *Fusion Science and Technology*. 2011, v. 59 (1T), p. 57-60.
11. Y. Li et al. // *Nuclear Fusion*. 2020 v. 60, p. 46029.
12. D. Nishijima et al. // *Journal of Nuclear Materials*. 2004, v. 329-333, p. 1029-1033.
13. M. Wirtz et al. // *Nuclear Materials and Energy*. 2017, v. 12, p. 148-155.
14. M. Tokitani et al. // *Journal of Nuclear Materials*. 2009, v. 386-388, p. 173-176.
15. I.E. Garkusha // *J. Phys. Conf. Ser.* 2015, v. 591, p. 012030.
16. V.A. Makhlay et al. // *Physica Scripta*. 2009, v. T138, p. 014060.
17. V.A. Makhlay et al. // *Physica Scripta*. 2014, v. T159, p. 014024.

Article received 15.11.2020

ПОВРЕЖДЕНИЯ ЧИСТОГО ВОЛЬФРАМА С РАЗНОЙ МИКРОСТРУКТУРОЙ ПРИ ПОСЛЕДОВАТЕЛЬНЫХ ПЛАЗМЕННЫХ НАГРУЗКАХ В КСПУ И LHD

С.С. Геращенко, О.В. Бирка, В.А. Махлай, М. Wirtz, Н.Н. Аксенов, И.Е. Гаркуша, Ю.В. Петров, С.В. Малихин, С.В. Суловицкий, S. Masuzaki, M. Tokitani, С.И. Лебедев, П.Б. Шевчук

Были оценены пороги растрескивания для образцов вольфрама с различной микроструктурой в процессе повторяющихся плазменных нагрузок КСПУ X-50. При нагрузках менее $0,1 \text{ МДж/м}^2$ на открытых поверхностях образцов вольфрама повреждений не наблюдается. Тем не менее трещины наблюдаются в объеме облученного образца вольфрама с продольной ориентацией зерен. Повышение тепловой нагрузки до $0,2 \text{ МДж/м}^2$ приводит к повреждению всех типов вольфрамовых мишеней. Наблюдаемые трещины распространяются в объеме в основном поперечно и параллельно облучаемой поверхности. Проанализировано влияние диверторной плазмы LHD на поверхность образцов вольфрама. Сравниваются результаты воздействия на образцы вольфрама с различной микроструктурой.

ПОШКОДЖЕННЯ ЧИСТОГО ВОЛЬФРАМУ З РІЗНОЮ МІКРОСТРУКТУРОЮ ПРИ ПОСЛІДОВНИХ ПЛАЗМОВИХ НАВАНТАЖЕННЯХ У КСПП І LHD

С.С. Геращенко, О.В. Бирка, В.О. Махлай, М. Wirtz, М.М. Аксенов, І.Є. Гаркуша, Ю.В. Петров, С.В. Малихін, С.В. Суловицький, S. Masuzaki, M. Tokitani, С.І. Лебедев, П.Б. Шевчук

Було оцінено пороги розтріскування для зразків вольфраму з різною микроструктурою в процесі повторюваних плазмових навантажень КСПП X-50. При навантаженнях менше $0,1 \text{ МДж/м}^2$, на відкритих поверхнях зразків вольфраму ушкоджень не спостерігається. Проте, тріщини спостерігаються в обсязі опроміненого зразка вольфраму з поздовжньою орієнтацією зерен. Підвищення теплового навантаження до $0,2 \text{ МДж/м}^2$ призводить до пошкодження всіх типів вольфрамових мішеней. Тріщини поширюються в обсязі в основному поперечно і паралельно до опромінюваної поверхні. Проаналізовано вплив диверторної плазми LHD на поверхню зразків вольфраму. Порівнюються результати впливу на зразки вольфраму з різною микроструктурою.